

Optimisation of Laser Groove Texturing of Cutting Tool Material using COMSOL Multiphysics

Harish P., Bharatish A*, Pavankumar Gurav

Department of Mechanical Engineering, RV College of Engineering, Bengaluru

Abstract

Introducing micro textures on the surface of cutting tools can significantly improve their cutting performance considerably. This paper reports the results of optimization of groove surface texturing on cemented carbide cutting tool. The effect of laser parameters such as laser power, scanning speed and beam radius were analyzed on ablation depth, thermal stress, and maximum temperature. The scanning speed was the major parameter affecting the ablation depth and maximum temperature. The hemispherical shaped ablation front was observed on the iso-surface corresponding to a minimum temperature of 337°C and highest temperature of 6060 °C. From response surface methodology based composite desirability technique, the optimal laser parameters of power 30 W, scanning speed 4 mm/s and beam radius of 25 μm were obtained for maximum ablation depth of 84.33 μm, minimum thermal stress of 982.2 MPa and minimum temperature of 4798.33 °C.

Keywords: *Micro textures, COMSOL, scanning speed, cutting tool*

1.0 Introduction

Laser machining is the material removal process in which laser beam is targeted on to the surface and material removal takes place by melting and vaporization. Laser texturing is a process of creating the patterns on the surface to improve properties such as thermal conductivity, adherence, friction, and enhancing the cutting tool characteristics with the lubrication.

Micro textures are produced on the cutting tool which improves the performance of the cutting tool by the hydrodynamic effect due to the lubrication between the texture and the machining chips. This also reduces the contact area, friction, and power. In cutting tool machineries, tungsten carbide is widely adopted because of its excellent properties such as high hardness, toughness and strength. Laser texturing of tungsten carbide can be performed to reduce the tool chip interface temperature and improve the tool life.

*Mail address: A. Bharatish, Assistant Professor, Department of Mechanical Engineering, RV College of Engineering, Bengaluru – 59
Email: bharatisha@rvce.edu.in, Ph: 9886445035

Some of the researchers have focussed on improving the performance of cutting tools using various methods. Deng Jianxin et al. [1] reported hybrid surface texturing with different geometrical characteristics on the rake face of tungsten carbide/Cobalt (WC/Co) carbide tools coated with molybdenum disulphide (MoS₂). The results showed the reduction in cutting forces at tool chip interface, cutting temperature, and coefficient of friction.

Bin le et al. [2] performed the numerical analysis of tool wear by using the Markov model which considers the contact stress, cutting temperature, and strain rate at the area between tool and work piece. Yunsong Lian et al. [3] investigated the effect of femto second laser textures created on rake face of uncoated cemented carbide tool and reported that the reduction in cutting temperature, cutting force and the friction coefficient at the tool–chip interface.

Xiuqing Hao et al. [4] investigated the effect of various shapes of micro and nano textures of the cutting tool produced using femtosecond laser. P Koshy et al. [5] reported the effect of micro holes made on rake face of cemented carbide tool using electric discharge machining. It was shown that self-lubrication of these micro holed tools significantly reduced friction between the tool chip interface and cutting forces when compared to the untextured tool. Ze Wu et al. [6] investigated the effect of micro textures while cutting Ti-6Al-4V and reported that the micro textured cutting tools can reduce the cutting temperature, cutting forces and cutting resisting forces and the actual tool-chip contact lengths by 5~25%, 2~10%, 5~20%, and 10% respectively. Deng et al. [7] created various geometrical textures on the rake face of cemented carbide inserts and filled the textures with solid lubricants. The dry cutting with these tools showed that reduction in friction at the tool-chip interface. Similar studies were reported to investigate the influence of surface texturing on the cutting performance of cemented tool using AdvantEdge FEM software [8 -10].

The effect of surface texturing on chip morphology, cutting force, and cutting temperature using DEFORM software is also reported [11-12]. Enomoto et al. [13] adopted an isotropic-textured cutting tool which was fabricated using electrical discharge machining and a significant reduction in feed and cutting forces in operation was demonstrated. Sugihara et al. [14] provided a type of nano-/micro-textured cutting insert which was fabricated using femtosecond laser and the face milling of aluminum alloy and showed that the textured surface exhibited superior anti-adhesive performance of workpiece materials. B Guimaraes et al. [15] analysed the effect of laser surface texturing on the wettability of WC-Co cutting tools

and reduced the tool-chip friction and wear rate at a contact angle of 33.5° , peak width of $250\ \mu\text{m}$, 3 laser passes resulting in a 27% reduction, when compared with an untextured cutting tool (45.8°). Bertolete et al. [16] reported rake face texturing by 40% decrease in friction force, a significant fall in chip deformation by about 21% and an improvement in the surface roughness.

From the review of literature [1-16], it was found that the effect of surface textures on rake and flank face of the cutting tools is reported using various sources such as lasers, electron beam and electrical discharge and so on. The cutting force, maximum temperature, friction and its effects on the cutting tool and various shape of textures were studied. However, before performing the actual experiments, there is a need to analyse the effect of laser texture parameters on the ablation depth and tool chip interface temperature in order to correlate with other texture responses. Hence the present paper focuses on establishing the correlation between the laser parameters and surface texturing responses by achieving a optimal combinations of laser texture parameters.

2.0 Experimental procedures

2.1 Experimental layout

The laser power, scanning speed and beam radius were selected as the laser parameters at three levels each according to L9 orthogonal array as shown in Table 1. Transient thermal analysis was performed using COMSOL Multiphysics to simulate the laser texturing process. The material properties considered for the simulation is as shown in Table 2.

Table 1. Experimental layout

Expt. No	Power [W]	Scanning speed [mm/s]	Beam radius [μm]
1	30	4	25
2	30	5	50
3	30	6	75
4	35	4	25
5	35	5	50
6	35	6	75
7	40	4	25
8	40	5	50
9	40	6	75

Table 2. Material properties

No	Property	
1	Density	15.88 Mg/m ³
2	Bulk Modulus	400GPa
3	Elastic Limit	530 MPa
4	Poisson Ratio	0.22
5	Shear Modulus	283GPa
6	Tensile Strength	530MPa
7	Young's Modulus	686GPa
8	Melting Point	2870 C
9	Specific Heat	292 J/Kg K
10	Thermal Conductivity	88 W/m K
11	Thermal expansion	5.5e-6/ K

Texturing is simulated by moving the laser heat source from the initial point of texture to final point of texture. For this purpose, the Gaussian heat flux for moving laser heat source is considered as given by Equation (1)

$$Q = \left(\frac{2P_0}{\pi R_b^2} \right) \exp \left\{ - \left(\frac{2R^2}{R_b^2} \right) \right\} \quad (1)$$

where,

$$R = \sqrt{((x - xf(t))^2 + (y - yf(t))^2)}$$

Q = Gaussian heat flux [W/m²], P₀ = Laser power [W], R_b = beam radius [μm], X and y are the coordinates in mm

Interpolation technique was adopted to achieve the path for moving heat source as indicated in the Table 3. With respect to scanning speed of 4mm/s, T(s) represents time in seconds, xf(t) and yf(t) represents the coordinates of laser beam at T(s). The co-ordinates are designed for the absolute movement of the laser beam.

Table 3. Interpolation table

T (s)	$xf(t)$	$yf(t)$
0	0	-14
1	0	-10
2	0	-6
3	0	-2
4	0	2
5	0	6
6	0	10
7	0	14

The square plate of thickness 5mm with the edge size of 50 mm is created using the Solid works and imported to the COMSOL window. The laser path of heating was also created using the Solidworks. The rectangular strip at the center of the square plate where the laser heat source is moved from point -15 mm to + 15mm. Tetrahedral and meshing is done by keeping mesh size as fine as shown in the Fig. 1.

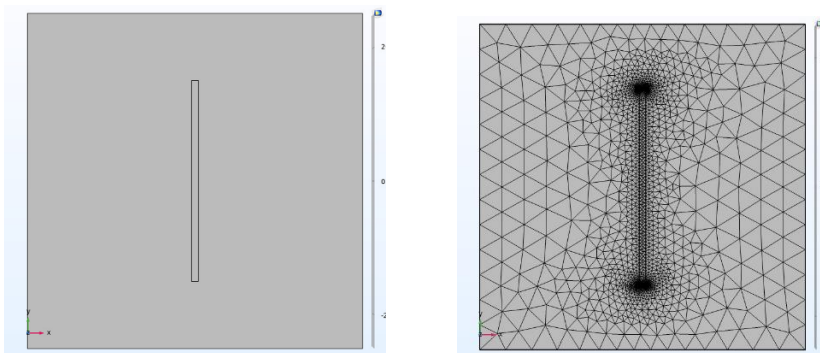


Fig. 1. The meshed geometry of laser track on the plate

3.0 Results and Discussion

3.1 Surface temperature

The melting point of the tungsten carbide is about 2870°C and moving laser heat source can remove the layer of material by melting and vaporization. The temperature values were minimum at the beginning and varies according to the time. At the end of 1s, the temperature is nearly around 4000 °C can be noted which is as shown in Fig 2. The ablation depth is located at the point where temperature exceeds than 2870°C. The hemispherical shaped ablation front was observed on the isosurface (Fig. 2) which lowest layer was at 337°C and center point of hemisphere at the top surface was at highest temperature of 6060 °C. The variation of

ablation depth versus temperature as shown in Fig. 3. The maximum stress was observed at 200 μm below the surface as shown in the Fig. 4. The simulation results for nine laser parametric conditions are as projected in Table 4. It was observed that maximum temperature of 12960°C corresponded to an ablation depth of 120 μm and the minimum temperature of 3130°C corresponded to 5 μm ablation depth.

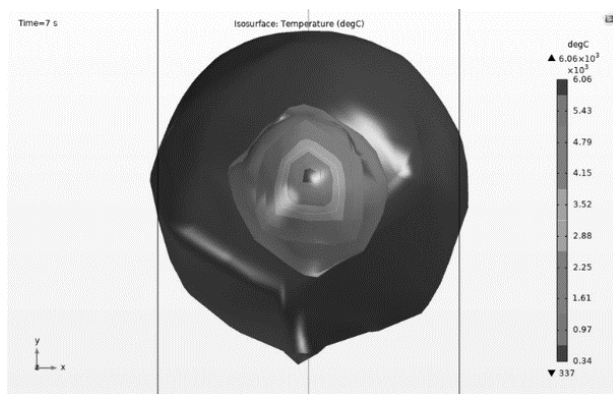


Fig. 2. Temperature distribution on the iso-surface

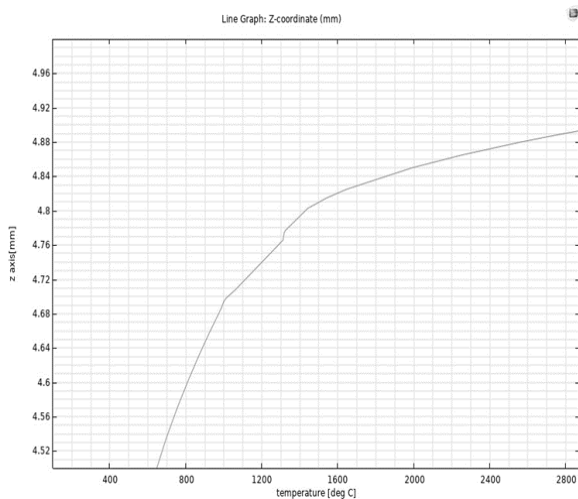


Fig. 3. Ablation depth vs temperature profile

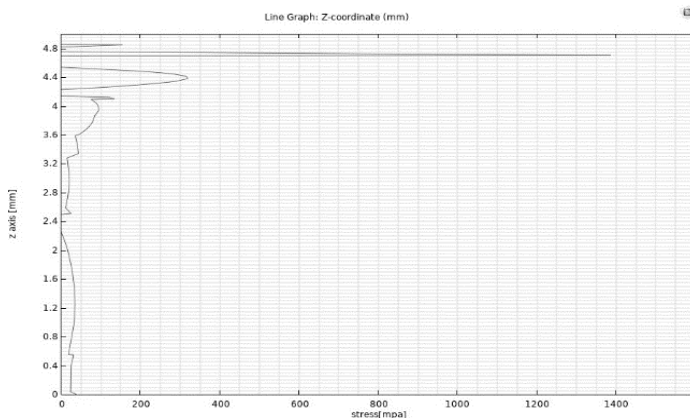


Fig. 4. Thermal stress distribution along the depth

Table 4. Simulation Results

Sl. No.	Power [W]	Scanning speed [mm/s]	Beam radius [μm]	Ablation depth [μm]	Max Temperature [$^{\circ}\text{C}$]	Max Thermal stress [MPa]
1	30	4	25	90	5120	1180
2	30	5	50	20	3230	500
3	30	6	75	2	2950	1150
4	35	4	25	110	6380	1350
5	35	5	50	30	3730	700
6	35	6	75	5	3130	1200
7	40	4	25	120	12960	1600
8	40	5	50	40	4550	850
9	40	6	75	15	3430	1300

3.2 Optimization of laser parameters

The effect of laser parameters on the ablation depth, maximum temperature and thermal stress is as shown in Fig. 5. Since the scanning speed was crossing the limiting value of 2.571, the ablation depth was significantly affected by scanning speed. The regression equation for the ablation depth (AD) is given by Equation (2).

$$AD (\mu\text{m}) = 217.2 + 2.10 (P) - 49.67 (Scp) + 0.113 (R_b) \quad (2)$$

Similarly, the maximum temperature was also significantly affected by scanning speed. The effect of power was slightly less than the scanning speed and the beam radius effect can be neglected for analysing the maximum temperature. Regression equation for the Maximum temperature is given by Eq 3.

However, the thermal stress was not significantly affected by any of the input parameters. The regression equation for the thermal stress is given by equation (4).

$$T_{max} (\text{°C}) = 3985 + 321 (P) - 2492 (Sc_p) + 45.6 (R_b) \quad (3)$$

$$\text{Thermal stress (Mpa)} = 346 + 30.7 (P) - 80 (Sc_p) + 1.47 (R_b) \quad (4)$$

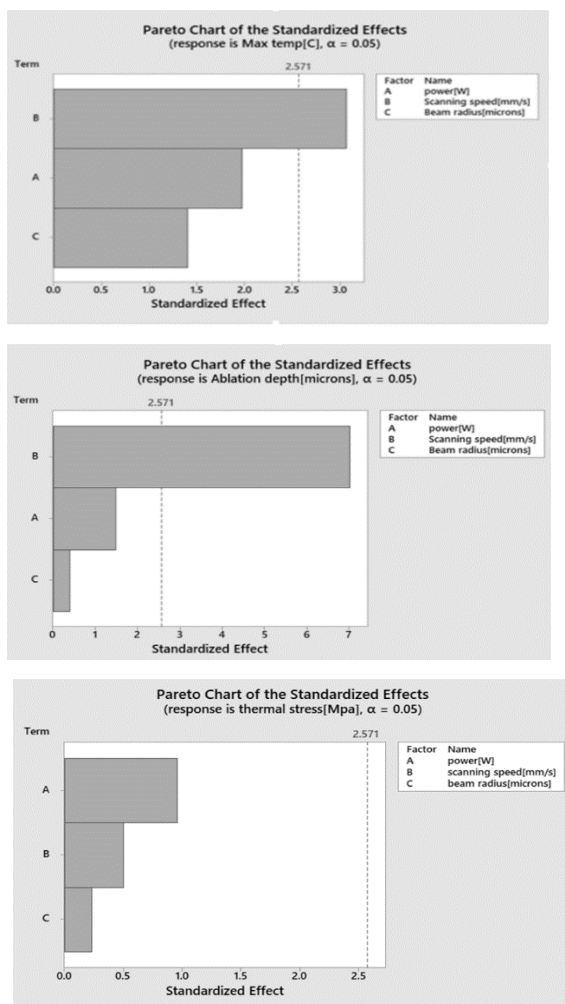


Fig. 5. Effect of laser parameters on a) Ablation depth, b) maximum temperature and Thermal stress

The laser parameters were optimized using Response Surface Methodology based composite desirability approach as shown in Fig. 6. The composite desirability was computed as the geometric mean of individual desirability of the responses. The responses with desirability value approaching towards unity would be acceptable whereas the responses with desirability value approaching towards zero would be

unacceptable. The maximum ablation depth of 84µm, reduced temperature of 4798.33°C and minimum thermal stress of 982 MPa corresponded to 30 W laser power, 4 mm/s scanning speed and 25 µm beam radius. The composite desirability of 0.683 was achieved which could be further improved by selection of wider range of laser parameters.

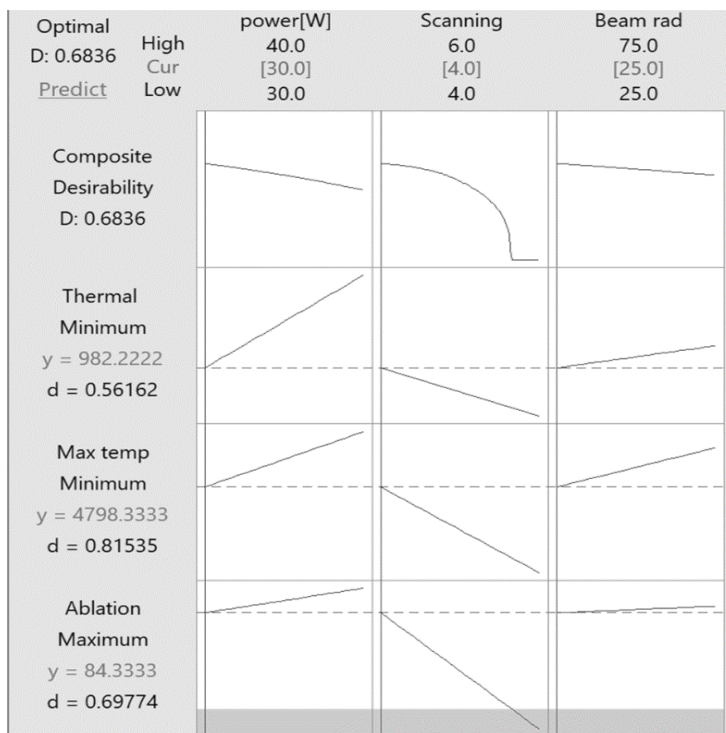


Fig. 6. Optimization using composite desirability

4.0 Conclusions

Laser surface texturing of carbide tools was simulated using COMSOL multiphysics package and it was observed that scanning speed was the major factor affecting the ablation depth and maximum temperature. As the scanning speed increased, both the ablation depth and maximum temperature decreased. The beam radius did not significantly affect any of the responses. The maximum ablation depth of 84µm, reduced temperature of 4798.33°C and minimum thermal stress of 982 MPa corresponded to 30 W laser power, 4 mm/s scanning speed and 25 µm beam radius. The composite desirability of 0.683 was achieved which could be further improved by selection of wider range of laser parameters.

References

1. D Jianxin, W Ze, L Yunsong, Q Ting, C Jie, Performance of Carbide Tools with Textured Rake-Face Filled with Solid Lubricants in Dry Cutting Processes, *International Journal of Refractory Metals and Hard Materials*, 30 (1), 164–172, 2012
2. B Li, A Review of Tool Wear Estimation Using Theoretical Analysis and Numerical Simulation Technologies, *International Journal of Refractory Metals and Hard Materials*, 35, 143–151, 2012
3. Y Lian, J Deng, G Yan, H Cheng, J Zhao, Preparation of Tungsten Disulfide (WS₂) Soft-Coated Nano-Textured Self-Lubricating Tool and Its Cutting Performance, *The International Journal of Advanced Manufacturing Technology*, 68, 2033–2042, 2013
4. Y Xing, J Deng, Z Wu, H Cheng, Effect of Regular Surface Textures Generated by Laser on Tribological Behavior of Si₃N₄/TiC Ceramic, *Applied Surface Science*, 265, 823–832, 2013
5. P Koshy, J Tovey, Performance of Electrical Discharge Textured Cutting Tools, *CIRP Annals*, 60 (1), 153–156, 2011
6. Z Wu, H Bao, L Liu, Y Xing, P Huang, G Zhao, Numerical Investigation of the Performance of Micro-Textured Cutting Tools in Cutting of Ti-6Al-4V Alloys.” *The International Journal of Advanced Manufacturing Technology*, 108, 463–474, 2020
7. J Deng, Z Wu, Y Lian, T Qi, J Cheng, Performance of carbide tools with textured rake-face filled with solid lubricants in dry cutting processes, *Int J Refract Met Hard Mater*, 30, 164–172, 2012
8. J Ma, N H Duong, S Lei, Numerical investigation of the performance of microbump textured cutting tool in dry machining of AISI 1045 steel, *J Manuf Processes*, 19, 194–204, 2015
9. G Liu, C Huang, R Su, T Özel, Y Liu, L Xu, 3D FEM simulation of the turning process of stainless steel 17-4PH with differently texturized cutting tools, *Int J Mech Sci*, 155, 417–429, 2019
10. S K Mishra, S Ghosh, S Aravindan, Performance of laser processed carbide tools for machining of Ti6Al4V alloys: A combined study on experimental and finite element analysis, *Precis Eng*, 56, 370–385, 2019
11. D M Kim, V Bajpai, B H Kim, H W Park, Finite element modeling of hard turning process via a micro-textured tool, *Int J AdvManuf Technology*, 78 (9–12), 1393–1405, 2015

12. D Arulkirubakaran, V Senthilkumar, V Kumawat, Effect of micro-textured tools on machining of Ti-6Al-4V alloy: An experimental and numerical approach, *Int J Refract Met Hard Mater*, 54, 2016
13. T Enomoto, T Sugihara, Improving anti-adhesive properties of cutting tool surfaces by nano-/micro-textures, *CIRP Ann Manuf Technol*, 59(1), 597–600, 2010
14. T Sugihara, T Enomoto, Development of a cutting tool with a nano/micro-textured surface-improvement of anti-adhesive effect by considering the texture patterns, *Precis Eng*, 33(4), 425–429, 2009
15. B Guimarães, D Figueiredo, C M Fernandes, F S Silva, G Miranda, O Carvalho, Laser machining of WC-Co green compacts for cutting tools manufacturing, *Int J Refract Met Hard Mater*, 81, 316–324, 2019
16. M Bertolete, P A Barbosa, R Machado, Effects of texturing the rake surfaces of cemented tungsten carbide tools by ultrashort laser pulses in machining of martensitic stainless steel, *Int J Adv Manuf Technol*, 98, 2653–2664, 2018